ANALYTIC PROPERTIES OF REGGE POLE TRAJECTORIES

Ya. I. AZIMOV, A. A. ANSEL'M, and V. M. SHEKHTER

A. F. Ioffe Physico-technical Institute, Academy of Sciences, U.S.S.R.

Submitted to JETP editor October 24, 1962

J. Exptl. Theoret. Phys. (U.S.S.R.) 44, 1078-1092 (March, 1963)

The motion of Regge poles at complex energies is studied for a Yukawa potential. It is found that the trajectories have complex (and real) branch points, due to collisions of pairs of poles. The position of these points is given explicitly for the case of weak coupling. For stronger coupling a qualitative description of the position of these branch points is given. With increasing coupling constant they leave the physical sheet and thereafter the trajectory can give rise to the appearance of bound states.

1. INTRODUCTION

In a previous paper of the authors [1] the behavior of Regge poles was studied for scattering by a Yukawa potential $V(r) = \alpha e^{-\mu r}/r$ for small α. The pole trajectories $l = l_i(k^2)$ were studied as the energy k^2 was varied along the real axis from $-\infty$ to $+\infty$. In the present paper we study the analytic properties of these trajectories for arbitrary complex k^2.

We find real as well as complex branch points, corresponding to the collisions of pairs of poles. All trajectories turn out to be different branches of a single analytic function. The existence of the branch points makes it possible to explain the open nature of the trajectories when k^2 is varied along the real axis from $-\infty$ to $+\infty$.[1] For the same reason it is not possible to assign definite quantum numbers to the trajectories that collide on the physical sheet. In the case of repulsion all poles collide on the physical sheet. On going over to the case of attraction we find that the collision point of the right-most pole moves off to the second sheet of the k^2 plane, and the pole becomes "normal." Its trajectory no longer has unphysical singularities, and a dispersion relation may be written for it over just one physical cut. As the coupling constant is increased the collision points (branch points) for other poles successively move off to unphysical sheets. The corresponding trajectories also become normal. Only to normal trajectories can one assign quantum numbers distinguishing one trajectory from another (the radial quantum number). As the coupling constant is further increased the normal trajectories give rise to the appearance of bound states. Thus, for any value of the coupling constant (for attraction) we have an infinite number of trajectories that collide on the physical sheet, and a finite number of normal trajectories some of which give rise to bound states.

It would seem that the indicated properties of the Regge pole trajectories are of a general character and will persist in a field theory also.

In Sec. 2 the general picture of the pole trajectories for complex k^2 is given. Its justification is given in Sec. 3, where we also find the position of the branch points in the k^2 plane. In Sec. 4 it is shown that with an appropriate choice of sheets it is possible to write dispersion relations for any of the trajectories with a certain finite number of additional cuts, which are not cuts for the amplitude.

The mechanism by which normal trajectories and bound states are produced as the coupling constant is increased is described in Sec. 5.

2. COMPLEX BRANCH POINTS. DESCRIPTION

In [1] the motion of Regge poles was studied as k^2 was varied along the real axis from $-\infty$ to $+\infty$. The limiting values of every trajectory (with the exception of the right-most one for attraction) for $k^2 = \pm\infty$ turned out to be different. For large values of k^2 the motion of the poles is described by the expression:[1]

$$l_n = -n - \frac{g\mu}{ik} P_{n-1}\left(1 + \frac{\mu^2}{2k^2}\right), \quad n = 1, 2, \ldots \qquad (1)$$

In the notation of reference 1 the coupling constant $g = -\alpha m/\mu$, for attraction $g > 0$; the numbering of the poles is shifted by unity. The function $l_n(k^2)$ does not have an essential singularity at infinity. Therefore the existence of different limits means that as one moves along the real axis from $k^2 = -\infty$ to $k^2 = +\infty$ and then returns to the point

of departure along a large semicircle one encircles some branch points. In what follows we shall find the position of these branch points explicitly for the case of weak coupling ($g \ll 1$). The noted open nature of the trajectories indicates, in essence, that the cuts from the branch points were drawn out to infinity so that the points $k^2 = -\infty$ and $k^2 = +\infty$ in going around the large semicircle are located on different edges of these cuts.

To clarify the entire picture we consider the pole trajectories as k^2 varies from zero to infinity along a ray with some phase: $k^2 = \kappa^2 \exp[i(\pi - \varphi)]$, $\kappa^2 = |k^2|$. The trajectories obtained in [1] correspond to $\varphi = 0$ and $\varphi = \pi$. In order not to cross any cuts while moving along a ray we draw the cuts from the branch points to infinity along straight lines with phases equal to the phase at the branch point (see Fig. 1).

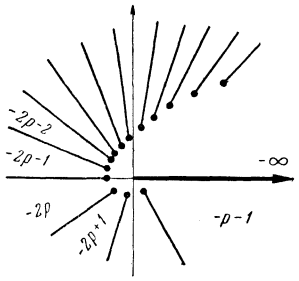

FIG. 1. Complex k^2 plane for the p-th upper trajectory in the case of attraction. The cuts are drawn to infinity. The limiting values (the quantity $-n$) of the trajectory for $|k^2| \to \infty$ in the various sectors are indicated.

For the sake of compactness we first give without proof the picture for the pole trajectory as κ^2 varies from infinity to zero for various values of φ from zero to π. This picture is shown in Fig. 2. Its justification will be given later. Figure 2a corresponds to the phase $\varphi = +0$, i.e., to motion in the k^2 plane along the upper edge of the cut which goes in Fig. 1 from the real branch point to $k^2 = -\infty$. For large κ^2 the poles oscillate near negative integer points; the corresponding segments in Fig. 2a are shown blackened. As κ^2 is decreased the poles collide in pairs and then move off into the complex plane and for $\kappa^2 \to 0$ reach the point $l = -\frac{1}{2}$. The pair of poles located for $\kappa^2 = \infty$ at the points $l = -2p$ and $l = -(2p + 1)$ ($p = 1, 2, \ldots$) for the case of attraction here considered collide to the left of the point $l = -2p$ and to the right of $l = -(2p + 1)$.[1)] In the case of weak coupling the collision point is close to $l = -2p$. With our choice

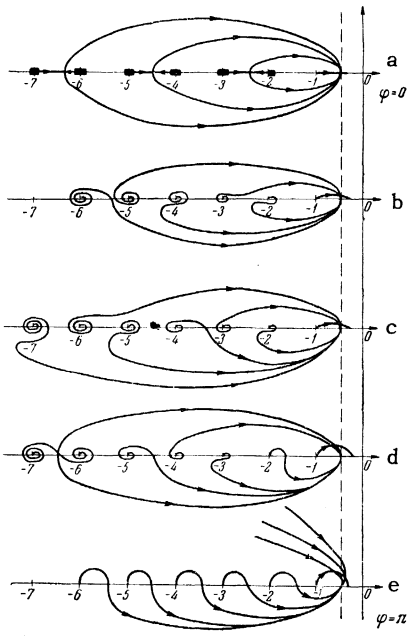

FIG. 2. Pole trajectory as k^2 varies along a ray with fixed phase ($\arg k^2 = \pi - \varphi$) from ∞ to 0. The phase φ increases from zero (Fig. 2a) to π (Fig. 2e).

of the edge of the cut the pole located at the odd point $-2p-1$ for $\kappa^2 = \infty$ moves after collision into the upper half-plane.

For a small positive value of the phase φ the motion of the poles in shown in Fig. 2b. The oscillatory segments of the trajectory near negative integer points are transformed into spirals, at that for a small value of the phase the spiral has as many loops as there were oscillations. With increasing φ the spiral gradually straightens out. The larger the number n of the trajectory the further such a trajectory moves from the point at which, for $\varphi = 0$, the collision of two neighbors took place. Moreover, the trajectory with even $n = 2p$, which for $\varphi = 0$ collided with its left neighbor ($n = 2p + 1$) now approaches its right neighbor and vice versa. In Fig. 2b this can be seen on the example of the trajectories with $n = 5$ and $n = 6$ the first of which collided with $n = 4$ and the second with $n = 7$ when φ was equal to zero. As the phase is further increased the trajectories collide in the upper half of the l plane.

The quantities $\tilde{\varphi}$ and $\tilde{\kappa}^2$ at which the collision occurs are equal to the phase and modulus of the branch point in the k^2 plane (see Fig. 1). As the phase passes through $\tilde{\varphi}$ we move over to the other side of the cut in the k^2 plane. At that the trajectory that previously went from the upper half-plane to the point $-n$ (-5 on Fig. 2b) now goes to the point $-n-1$ (-6 on Fig. 2b). The lower trajectory, on the contrary, instead of the point $-n-1$ reaches the point $-n$. The corresponding situation is shown in Fig. 2c. Consequently, after collision the limiting value for $\kappa^2 = \infty$ for the upper

[1)] As was noted in [1] for $k^2 \to 0$ these trajectories are described by

$$l = -\tfrac{1}{2} \pm 2\pi i p/[\ln(\mu^2/k^2) + i\pi], \quad p = 1, 2, \ldots$$

The plus (minus) sign refers to the trajectories which reach the point $l = -1/2$ from the upper (lower) half-plane. In what follows we refer to these trajectories as "upper" and "lower" respectively.

trajectory is shifted to the left by unity, and for the lower trajectory to the right by unity. We note that the number of half loops of the spiral near the given integer point decreases by one after collision.

Let us follow the fate of the upper trajectory which goes in Fig. 2a, 2b into the point $l = -5$, and in Fig. 2c into $l = -6$. As the phase is increased it approaches now the lower trajectory that goes to the point $l = -7$. The moment of their collision is shown in Fig. 2d. It should be noted that the lower trajectory fell into the point $l = -7$ as a result of a collision that occurred at a smaller phase; at $\varphi = 0$ it went to $l = -8$.

As the phase is increased still further the story repeats itself. The spirals near the integer points straighten out, the trajectories collide, the upper trajectories are shifted after collision to the left, the lower to the right.

As the phase changes from zero to π each of the upper trajectories collides in succession with each of the lower trajectories whose limiting points for $\varphi = 0$ were to the left of it. The number of such trajectories is infinite. Since at each collision the limiting value changes by unity, for $\varphi \to \pi$ the limiting value of all upper trajectories goes to $-\infty$.

The lower trajectories collide with all their right upper neighbors. If for $\varphi = 0$ the limiting value of the lower trajectory was $l = -2p$, then the number of such neighbors was $p-1$. Therefore for $\varphi = \pi$ the limiting value is $l = -2p + (p-1) = -p - 1$. The picture arising for $\varphi = \pi$ is shown in Fig. 2e. This is precisely the picture that we have arrived at previously [1] when considering positive k^2. For negative k^2 the motion of the poles corresponded to the picture in Fig. 2a. The open nature of the trajectories noted in [1] corresponds to the shift of the limiting values ($\kappa^2 = \infty$) as φ varies from zero to π.

Up to now we have varied the phase from $+0$ to π. This corresponded to the upper half of the k^2 plane [$k^2 = \kappa^2 \exp\{i(\pi - \varphi)\}$]. In the lower half plane φ varies from -0 to $-\pi$. It is easy to understand that in that case the motion of the poles is described in precisely the same way as for positive φ if in the preceding discussion one interchanges everywhere the words "upper" and "lower" (trajectory, half-plane).

As was already remarked above, the values of k^2 at which pole collision takes place are determined by the positions of branch points in the k^2 plane. If one considers the upper trajectory which has the limiting value $l = -2p-1$ for $\kappa^2 = \infty$, $\varphi = +0$, one concludes from the above discussion that it has one real branch point, an infinite number of branch points in the upper half-plane (corresponding to the infinite number of collisions for $0 < \varphi < \pi$) and $p-1$ branch points in the lower half-plane of k^2. The latter is connected with the fact that an "upper" trajectory behaves in the lower half-plane in the same way as the "lower" trajectory in the upper half-plane of k^2. The indicated branch points and cuts for the upper trajectory, as well as the limiting values of the trajectory (at $\kappa^2 = \infty$) in the various sectors, are shown in Fig. 1. There is also shown in Fig. 1 the physical cut running from $k^2 = 0$ along the positive semi-axis. The corresponding picture for a lower trajectory may be obtained from Fig. 1 by interchanging the upper and lower half-planes, i.e., by the operation of complex conjugation.

Let us note that in the case of repulsion the picture of the singularities is the same as in Fig. 1, except that the limiting values are shifted by unity (see [1]).

3. COMPLEX BRANCH POINTS. JUSTIFICATION

a) Spirals.

Near negative integer points the motion of the poles is described by Eq. (1). For a fixed value of the phase $0 < \varphi < \pi$ [$k^2 = \kappa^2 \exp\{i(\pi - \varphi)\}$] and for κ^2 varying from infinity to $\kappa^2 \ll \mu^2$ the Legendre polynomial P_{n-1} continuously changes its phase from zero to $-(\pi - \varphi)(n-1)$. At that the modulus $|k^{-1}P_{n-1}(1 + \mu^2/2k^2)|$ increases from zero up to a finite value. It therefore follows that in the neighborhood of the integer point the trajectory is described by a spiral with the number of half loops equal to $(n-1)(1-\varphi/\pi)$. As $\varphi \to \pi$ the spiral straightens out. For $0 > \varphi > -\pi$ the polynomial P_{n-1} has in the region $\kappa^2 \ll \mu^2$ the phase $+(\pi + \varphi)(n-1)$. Consequently on passing into the lower half-plane the spiral changes its direction and for $\varphi \to -\pi$ straightens out, as before.

b) With increasing φ upper trajectories go left, lower go right.

For sufficiently small κ^2 Eq. (1) ceases to be valid. In that region, as was shown in [1], one must use the equation

$$\xi_l \left(\frac{k^2}{\mu^2} e^{-i\pi}\right)^{l+1/2} = -\sin l\pi, \quad \xi_l = g\,\frac{\sqrt{\pi}\,\Gamma(-l-1/2)}{\Gamma(-l)}. \qquad (2)$$

As k^2 varies along the negative semi-axis Eq. (2) gives rise to motion of poles in the upper and lower half-planes along curves close to circular arcs. [1] This is obtained if one ignores the l dependence of $\ln \xi_l$ and takes into account in $\sin l\pi$ only the growing exponential. It is not hard to see

that under the same assumptions but for k^2 varying along a ray with a given phase the equation for the trajectory in the upper half-plane has the form

$$\left(\mathrm{Re}\left(l+\tfrac{1}{2}\right)+p\frac{\pi}{\pi-\varphi}\right)^2+\left(\mathrm{Im}\,l-\frac{1}{2(\pi-\varphi)}\ln 2\xi_l\right)^2 = p^2\frac{\pi^2}{(\pi-\varphi)^2}+\frac{\ln^2 2\xi_l}{4(\pi-\varphi)^2}, \qquad p=1,2,\ldots \tag{3}$$

The meaning of the number p here, as in the rest of this Section, is explained in the first footnote.

For $\varphi = 0$ this equation coincides with Eq. (11) of [1] and describes the upper trajectory which reaches the real axis between the points $l = -2p$ and $l = -2p-1$ (see Fig. 2a). As φ increases the radius of the circle increases and the point of intersection of the circle with the real axis moves to the left. Although in the immediate neighborhood of the real axis Eq. (3) is not correct it does describe the major part of the trajectory and therefore correctly reflects the nature of its shift. As $\varphi \to \pi$ the point at which the upper trajectory reaches the real axis moves to $-\infty$ and the circle is transformed into the straight line described in [1].

As φ varies from zero to $-\pi$ (k^2 in the lower half-plane) the radius of the circle and the position of the point at which it intersects the real axis are decreased by a factor two.

It is not hard to deduce from Eq. (2) that the equation for the "lower trajectory is obtained from Eq. (3) by the replacements $\varphi \to -\varphi$ and $\mathrm{Im}\,l \to -\mathrm{Im}\,l$. This means that the "lower" trajectories behave as k^2 varies in the upper half-plane analogously to the upper trajectories when k^2 varies in the lower half-plane. As φ increases from zero to π they are shifted to the right.

c) Collision of trajectories.

The position of the points of collision of two poles may be determined by solving simultaneously Eq. (2) and the equation obtained from Eq. (2) by differentiation with respect to l. Let us take logarithms of Eq. (2) choosing the phase to correspond to the upper p-th trajectory ($-2\pi ip$). If we now differentiate the resultant equation with respect to l and eliminate from both equations k^2 we obtain the following equation for the collision points of the upper p-th trajectory in the l plane:

$$\ln\xi_l+\pi\left(l+\tfrac{1}{2}\right)\mathrm{ctg}\,l\pi=\ln\cos\left(l+\tfrac{1}{2}\right)\pi-2\pi ip. \tag{4}*$$

Values of k^2 at which collisions occur are defined by the equation

$$\ln\left(\frac{k^2}{\mu^2}e^{-i\pi}\right)=\pi\,\mathrm{ctg}\,l\pi. \tag{5}$$

We solve Eq. (4) under the assumption that $\ln \xi_l$ is a large number. It is obvious that in that case l must be near an integer so that $\cot l\pi$ and $\ln\cos(l+\frac{1}{2})\pi$ will be large. Setting

$$l=-N-\delta, \tag{6}$$

and throwing away terms of order unity we find

$$\ln\xi_l+\frac{1}{\delta}\left(N-\tfrac{1}{2}\right)=\ln\delta+i\pi(N-2p). \tag{7}$$

The term $i\pi N$ in Eq. (7) represents the phase of $\cos(l+\frac{1}{2})\pi$. For $l = -\frac{1}{2}$ the phase is chosen to be zero; as the pole moves in the upper half-plane to the point to the left of $l = -N$ the term $\cos(l+\frac{1}{2})\pi$ acquires the phase $N\pi$. It is seen from Eqs. (4) and (7) that two upper trajectories with different numbers p and p′ cannot collide with each other and, consequently, an upper trajectory can only collide with a lower one.

The equation for the collision points of a lower p-th trajectory is obtained from Eq. (4) by the replacement $p \to -p$. It is not hard to see that in that case the phase of $\cos(l+\frac{1}{2})\pi$ at $l = -N-\delta$ is equal to $-N\pi$. Therefore the equation for the collision of a lower trajectory of number p′ differs from Eq. (7) in the neighborhood of the integer point $-N$ in the last term, which in the present case is given by $-i\pi(N-2p')$. It is therefore clear that the collision between the p-th upper and p′-th lower trajectories occurs in the neighborhood of the point $-N = -(p+p')$. This point lies nearly halfway between the limiting points $(-2p-1)$ and $(-2p')$ to which the corresponding poles go as $k^2 \to -\infty$. Consequently the equation for the collision of the p-th upper and p′-th lower trajectories in the l plane is given by

$$\ln\xi_l+\frac{1}{\delta}\left(p+p'-\tfrac{1}{2}\right)=\ln\delta+i\pi(p'-p). \tag{8}$$

From here one has with logarithmic accuracy ($\delta \ln\delta \ll 1$):

$$l=-(p+p')-\delta=-(p+p')-\frac{p+p'-1/2}{\ln(1/\xi_l)+i\pi(p'-p)}. \tag{9}$$

Substituting Eq. (9) into Eq. (5) we find the value of k^2 at which the collision takes place, i.e., the position of the branch point:

$$\frac{k^2}{\mu^2}=\frac{\varkappa^2}{\mu^2}e^{i(\pi-\varphi)}=\exp\left\{\frac{\ln\xi_l}{p'+p-1/2}+i\left(\pi-\frac{p'-p}{p'+p-1/2}\pi\right)\right\}. \tag{10}$$

It is seen from Eq. (10) that the upper trajectory of number p collides with all lower trajectories, located to the left of it (p′ > p), in the upper half

*ctg = cot.

of the k^2 plane ($\varphi > 0$). The collision with $(p-1)$ right lower neighbors ($0 < p' < p$) occurs in the lower half of the k^2 plane. The collision with the lower trajectory of the same number $p' = p$ occurs on the real axis, as was already noted in [1]. These considerations also make clear what the situation is for the lower trajectories.

In the case of repulsion all equations remain valid with ξl replaced by $-\xi l$ and p by $p - 1/2$.

d) Position of branch points.

The following properties of the branch points of the p-th upper trajectory (Fig. 1) can be seen from Eq. (10). In the weak coupling approximation the branch points lie at $\kappa^2 \ll \mu^2$. As p' increases κ^2 increases and for $\kappa^2 \sim \mu^2$ Eq. (10), derived under the assumption $\kappa^2/\mu^2 \ll 1$, ceases to be correct. Consequently we are unable to directly determine the position of the infinite number of branch points corresponding to collisions with very distant trajectories [$p' \gtrsim \ln(1/\xi l)$]. The magnitude of the phase $\varphi = (p'-p)\pi/(p'+p-1/2)$ also increases with increasing p' and approaches π still within the region of applicability of the theory for $p' \gg p$. This means that although both the real and imaginary parts of the position of the branch point increase with increasing p', the imaginary part increases somewhat slower so that an accumulation of such points occurs at $\varphi = \pi$. Let us note that although, as has been already remarked, we are not able to determine the modulus of k^2 for very large values of p' it can be asserted that for $\varphi \to \pi$ the branch points do not accumulate at a finite point on the real axis. The latter would indicate the existence of a singularity for real $k^2/\mu^2 \sim 1$, which was not found in [1]. Let us also note that the branch points cannot accumulate at $k^2 = 0$ either, since in the neighborhood of that point Eq. (10) is applicable and it shows no such accumulation. Consequently the branch points move off to infinity with a phase equal to π.

4. DISPERSION RELATION FOR REGGE TRAJECTORIES

In the previous Section it was shown that the trajectories of Regge poles have an infinite number of branch points at which the poles collide in pairs. This means that all the trajectories form a single analytic function, of which they are different branches. The choice of the branch of the analytic function is fixed by introduction of cuts from the branch points. Up to now we have drawn all cuts in the k^2 plane out to infinity. At that on each sheet, determining a separate trajectory, one had an infinite number of complex branch points and cuts. The representation of the function on this sheet in the form of a sum of dispersion integrals over an infinite number of cuts is most inconvenient. In particular, such a sum would have to, apparently, converge nonuniformly in order to assure the existence of different limits of the trajectory for $k^2 \to \infty$ along different directions. For this reason it makes sense to choose the sheets in a different way, namely to draw the cuts in such a way that on any finite sheet there remain only a finite number of branch points.

In this section we show that this aim can be achieved by drawing all the cuts in the k^2 plane from the branch points to zero. When the cuts were drawn out to infinity the behavior of the poles in the neighborhood of $k^2 = 0$ was given by the equation

$$l + 1/2 = \pm 2\pi i p/[\ln(\mu^2/k^2) + i\pi],$$

valid when the point zero is approached from any direction. It was therefore convenient to label the trajectory by the number p, which determines its behavior as $k^2 \to 0$, and follow the variation of its limiting value at infinity as a function of the phase φ. Now, when the cuts are drawn towards zero, the situation is reversed. At infinity there remains only the physical cut and the limiting values of each trajectory are the same in any direction.

The behavior of the trajectory in the neighborhood of infinity is described by Eq. (1). In accordance with this formula it is convenient to label the trajectory by the number n, which determines its limiting behavior at infinity $l = -n$. It is easy to see that the behavior in the neighborhood of zero now depends on the phase of k^2. Indeed, as can be seen from the results in Sec. 1, to a given limiting point $l = -n$ as the phase of k^2 is varied there arrive alternately upper and lower trajectories with different values of p. In the case of attraction, as φ varies from $+0$ to π, there arrive at the even point n in succession the following trajectories: a lower with $p = n/2$, an upper with $p = n/2 - 1$, a lower with $p = n/2 + 1$, an upper with $p = n/2 - 2$, etc., down to a lower with $p = n - 1$. To the point with odd n there arrive in succession: an upper with $p = (n-1)/2$, a lower with $p = (n-1)/2 + 1$, an upper with $p = (n-1)/2 - 1$, etc., down to a lower trajectory with $p = n - 1$. As φ varies from -0 to $-\pi$ one must interchange in the above description the words "upper" and "lower."

If one fixes the character of the trajectory at infinity, i.e., the number n, then the trajectory that departs from this point is described in the neighborhood of the point zero by an expression

of the form

$$\pm 2\pi ip/[\ln(\mu^2/k^2) + i\pi],$$

where the ± sign refers to the upper and lower trajectories respectively, and p changes with varying φ in the manner described above. The change in the sign and magnitude of p takes place in a jump as the phase goes through the value corresponding to the branch point. This means that on going through such a phase we pass to the other side of the cut drawn from the branch point to zero. Since for a given value of n the quantity p takes on a finite number of values there can be on the sheet under consideration only a finite number of branch points. The position of these branch points is determined by Eq. (10). At that the quantity $r = p' - p$ is, in effect, equal to the number of the branch point: for a trajectory with a given value of n the quantity $r = 0, \pm 1, \ldots \pm(n-2)$. The quantity $p' + p$ is even or odd, according as r is even or odd, and equal to n or $n-1$. Thus the trajectory with the number n has in the k^2 plane one real and $(n-2)$ complex conjugate pairs of branch points.

Since the distance of the branch point from the origin in the k^2 plane is determined by the quantity $p' + p$ it follows that all the branch points for a given trajectory now lie on the circumference of two circles whose radii increase with increasing trajectory number n. The branch points due to the collisions with the right neighbor of number $n-1$ lie on one of these circumferences $(p + p' = n-1)$, and those due to collisions with the left neighbor of number $n+1$ lie on the other $(p + p' = n)$.

The position of these points and cuts is shown schematically in Fig. 3. Also shown are the values $\pm p$ that determine the behavior of the trajectory near $k^2 = 0$ in the various sectors. The trajectories which for $\varphi = \pi$ went to infinity in Fig. 2e correspond to $n = \infty$ and cannot be pictured in a figure of the type of Fig. 3.

The passage from the cuts shown in Fig. 3 to those in Fig. 1 is, of course, connected with the passage to other sheets. Each of the cuts in Fig. 3 should at that be deformed as follows. From the point $k^2 = 0$ the cut now goes along the positive real axis to infinity and then from infinity in to the branch point along a ray with a phase equal to the phase of the branch point. It is not hard to understand that when the cuts are so deformed an infinite number of branch points is uncovered, which accumulate in phase to $\varphi = \pi$ and which previously lay on more distant sheets.

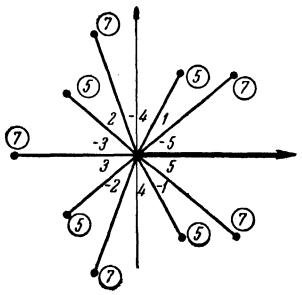

FIG. 3. Complex k^2 plane for the trajectory with $n = 6$. The cuts are drawn to zero. In the various sectors the values $\pm p$, determining the behavior of the trajectory for $k^2 \to 0$, are indicated $[l(k^2) = -1/2 \pm 2ip\pi/[\ln(\mu^2/k^2) + i\pi]$, the ± sign corresponding to upper or lower trajectory]. The number of the trajectory responsible for the branch point as a result of collision is shown encircled.

It may be noted that the new way of drawing the cuts makes it possible to establish a connection between the trajectories for a Yukawa potential and the Coulomb trajectories which are obtained by letting $\mu \to 0$. In this limit Eq. (1) goes over into the exact Coulomb formula, and the branch points together with the cuts collapse to zero according to Eq. (10). The same limit with the cuts drawn as in Fig. 1 results in the complex k^2 plane being cut into an infinite number of unconnected sectors.

The choice of the sheet described in this section allows one to write a dispersion relation for any Regge trajectory in terms of a sum of dispersion integrals over the complex cuts shown in Fig. 3.

The branch points of Regge trajectories, corresponding to collisions of poles, do not, of course, constitute singularities of the partial wave amplitudes. Therefore the choice of the sheet for the study of the analytic properties of an individual trajectory has no effect on the properties of the amplitude.

A study of the case of repulsion leads to analogous conclusions. The position of the branch points is determined, as before, by Eq. (10) with the replacements $p \to p - \frac{1}{2}$, $p' \to p' - \frac{1}{2}$ and $\xi_l \to -\xi_l$. For a trajectory with a given number n the quantity $r = p' - p$ takes on the values $r = 0, \pm 1, \ldots \pm(n-1)$. The quantity $p + p'$ is even or odd according as r is even or odd and equal to n or $n+1$. The number of complex conjugate pairs of branch points is in this case equal to $(n-1)$.

5. INCREASE IN COUPLING CONSTANT AND APPEARANCE OF BOUND STATES

So far we have considered the case of arbitarily weak coupling. It is of interest to understand how

the picture of the motion of the poles changes with increasing coupling constant, and, in particular, how do bound states appear. Qualitatively new properties of the trajectories may already be studied in the next order of perturbation theory. It is convenient here to consider the region of small k^2 values. The equation for the motion of the poles in this region is obtained in the Appendix. Accurate to terms of order $\sim g^2$ it has the form

$$\xi_l\left(\frac{k^2}{\mu^2}e^{-i\pi}\right)^{l+1/2}\left[1+\frac{g}{l+1/2}\left(\frac{1}{2^{2l+1}}-1\right)\right] = -\sin l\pi\left(1-\frac{g}{l+1/2}\right). \quad (11)$$

As was already remarked previously,[1] along with the poles described above Eq. (11) gives rise to a new type of pole, which for $k^2 = 0$ ends up not at $l = -1/2$ but at some other real point $l_0 < -1/2$. The position of this point corresponds to the vanishing of the expression in the square brackets [since $(k^2\mu^{-2}e^{-i\pi})^{l+1/2} \to \infty$ as $k^2 \to 0$] and, consequently, depends on g. For small g this point lies at a distance $|l_0| \sim \ln(1/g)$ from zero. It can be verified that higher orders of perturbation theory have a small effect on the quantity l_0 (see Appendix). As g increases $|l_0|$ decreases. The existence of poles of this type was first discovered in the work of Ahmadzadeh, Burke, and Tate.[2] In the case of repulsion there are no such poles.

Equation (11) also has an infinite number of solutions which for $k^2 = 0$ end up at certain points that come in complex conjugate pairs. All these points lie to the left of l_0. In the following we consider only the trajectory that ends up for $k^2 = 0$ at the real point l_0.

Let us study the trajectory of the new pole (referred to in the following as the N-trajectory) for real negative values of k^2, and also the influence of this pole on the motion of the other poles. It follows from Eq. (11) that as $-k^2$ ($k^2 < 0$) increases from zero the N-pole moves out from l_0 towards the nearest even point. In Fig. 4a we show the situation when $-6 < l_0 < -5$. As k^2 varies from zero to $-\infty$ the N-pole moves from $l = l_0$ to $l = -6$. The character of the trajectories lying to the right of l_0 is qualitatively the same as in the absence of the N-pole. Indeed, Eq. (11) differs from Eq. (2) only by the factor $\{1 + [g/(l + 1/2)]\times(2^{-2l-1} - 1)\}$ which in this region simply makes for a smaller effective value of ξ_l. Therefore, as before, the fifth pole collides with the fourth, and the third with the second. The story is different for

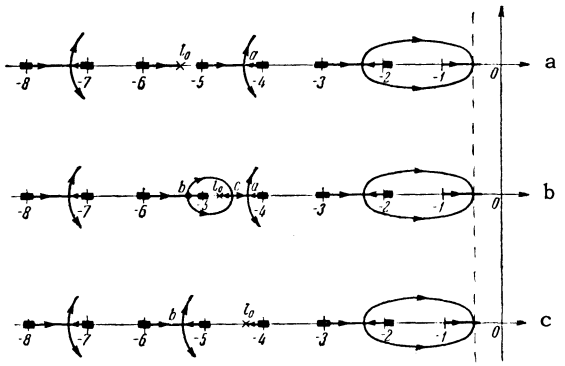

FIG. 4. Pole trajectories for real negative k^2 after the arrival of the N-pole; l_0 – its limiting value for $k^2 \to 0$. The coupling constant increases from Fig. 4a to Fig. 4c.

the poles that lie to the left (at $k^2 = -\infty$) of l_0. For $l < l_0$ the expression in the square brackets in Eq. (11) is negative which changes attraction into effective repulsion, and therefore to the left of l_0 the even left and odd right poles collide, as is normally the case for repulsion.[1]

With increasing g l_0 moves to the right. When l_0 has moved sufficiently far to the right of the point -5 the situation depicted in Fig. 4c is created. Now as k^2 varies from zero to $-\infty$ the N-pole moves from $l = l_0$ to $l = -4$; to the right of it the second and third poles collide, to the left of it the fifth and sixth poles collide.

The question arises: how does the transition from the picture shown in Fig. 4a to that shown in Fig. 4c take place? Equation (11) allows one to answer this question. Because of lack of space we do not give details but only describe the result.

When l_0 passes through the point -5 we have the situation depicted in Fig. 4b. As k^2 varies from $-\infty$ the fifth and sixth trajectories move towards each other, collide at the point b and diverge into the complex plane. The point b corresponds to the point also so labeled in Fig. 4c. As $-k^2$ is further decreased the fifth and sixth trajectories do not, however, move towards $l = -1/2$, but return instead to the real axis and collide at the point c. Thereafter they diverge along the real axis; one pole ends up for $k^2 = -0$ at l_0 and is the N-pole, the other moves towards the fourth pole and collides with it at the point a (which corresponds to just such a point in Fig. 4a). After this collision as $k^2 \to 0$ two poles go through the complex plane to the point $l = -1/2$.

Figure 4b differs from Fig. 4a in that it contains two additional real collision points (b and c). For $l_0 < -5$ these points were located in the complex plane and corresponded to the collision of the

fifth and sixth trajectories for complex k^2. Their first appearance on the real axis occurs at the point -5 for that value of g for which l_0 is also equal to -5. With increasing g l_0 moves to the right and the points b and c diverge in opposite directions.

As g further increases the point c approaches the point a. After their coincidence the fourth trajectory becomes an N-trajectory (for $k^2 = 0$ it ends up at l_0), and the fifth and sixth trajectories after colliding at the point b go through the complex plane to $l = -\frac{1}{2}$. We arrive at Fig. 4c.

It must be noted that the collisions at the points a, b, and c and in the intermediate region take place when $-k^2/\mu^2 \sim 1$, when Eq. (11) is, strictly speaking, inapplicable. It is to be expected, however, that the qualitative features described by us are valid.

As g continues to increase the point l_0 continues to shift to the right. As l_0 passes through the point -3 a process analogous to that described above takes place after which the limiting position of the N-trajectory for $k^2 \to -\infty$ becomes equal to -2 and does not change anymore.

If terms of higher order in g are taken into account in the equations for the trajectories then one finds other N-poles lying to the left of the first N-pole. The last limiting position for $k^2 \to -\infty$ of the second N-pole is equal to -3. For the following N-poles it is -4, -5, etc.

We have analyzed the motion of the poles for negative k^2. The case of positive and complex k^2 turns out to be more complicated. Several trajectories of N-poles for positive k^2, obtained by numerical calculations, are shown in the work of Ahmadzadeh, Burke, and Tate.[2] We shall not describe the trajectories of the poles but will discuss only their analytic properties in k^2 as a function of g. For simplicity we limit ourselves to poles with smallest numbers.

In Fig. 5 is shown the complex k^2 plane for the second trajectory ($n = 2$). Before the arrival of l_0 at the point -3 the second trajectory has one real branch point corresponding to the collision with the third pole (Fig. 5a). After the limiting value l_0 of the N-pole passes through the point $l = -3$, analogously to what has been described above for the fifth and sixth trajectories (Fig. 4b), the third and fourth trajectories undergo double collisions to the left and right of the point $l = -3$, prior to colliding with the second trajectory. Both collision points are, obviously, root type branch points in the k^2 plane. It is easy to understand that after going around both branch points in the same direction the fourth trajectory, which was moving with decreasing $-k^2$ along the real axis from left to right, continues to move in that direction, while the third trajectory moves along the real axis to the left. Therefore the third trajectory falls into the point l_0 whereas with the second trajectory collides the fourth. This means that for l_0 somewhat larger than -3 Fig. 5a remains correct, however the branch point corresponds now to the collision with the fourth trajectory.

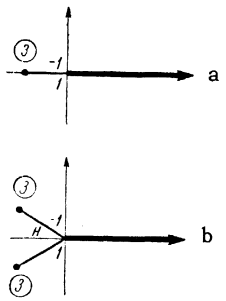

FIG. 5. Complex k^2 plane for the trajectory with $n = 2$ for various coupling constants; a – prior to the arrival of the N-pole, b – after the arrival of the N-pole but before the disappearance of the branch points onto the unphysical sheet.

As g increases further, as was explained above, the collision points a and c (displaced now relative to Fig. 4b by two units to the right) coincide, and thereafter the second trajectory goes for $k^2 \to -0$ to the point l_0. This means in the complex k^2 plane that instead of one real branch point there appear two complex conjugate branch points, so that there exists a sector near the negative real axis in which the second trajectory represents an N-pole with the limiting value l_0 (Fig. 5b). In order to understand how one real branch point corresponding to collision with the fourth trajectory is replaced by two complex conjugate ones, corresponding to collisions with the third trajectory, one must turn to a discussion of the third and fourth trajectories. For the sake of conciseness we conclude first the discussion of the second trajectory. As g increases the complex branch points approach the positive real axis and disappear through the physical cut. At the moment of their disappearance the second trajectory collides with the third for real positive k^2. A case of that type is shown in [2] in Fig. 4.

For yet larger values of g the plane of the second pole contains only the physical cut, the trajectory is closed as k^2 varies from $-\infty$ to $+\infty$, remaining real for all $k^2 < 0$ and lying in the upper half-plane for $k^2 > 0$. In this sense the trajectory is "normal," one can write for it a dispersion relation with only the single physical cut. As g increases further l_0 continues to shift to the right. As l_0 passes through $-\frac{1}{2}$ the equation defining l_0 changes. For $l_0 < -\frac{1}{2}$ the point l_0 corresponds

to the vanishing of the left side of Eq. (11) or rather of the more precise Eq. (A.8) obtained without simplifications arising from perturbation theory. For $l_0 > -\frac{1}{2}$ the quantity $(k^2/\mu^2)^{l+1/2} \to 0$ as $k^2 \to 0$ and it is then necessary to equate to zero the right side of the same equation. It is clear from the formulas in the Appendix that the passage through $l_0 = -\frac{1}{2}$ with increasing g proceeds continuously so that for $l_0 = -\frac{1}{2}$ the left and the right sides of Eq. (A.8) vanish simultaneously (both sides should be first multiplied by $l_0 + \frac{1}{2}$ to remove the singularity at that point). When l_0 passes through non-negative integer values bound states are produced. It is interesting to note that the creation of a normal trajectory occurs for values of g smaller than needed for the creation of bound states.

Let us investigate now the k^2 plane for the third trajectory (n = 3). As long as the N-pole is sufficiently far to the left the plane looks as shown in Fig. 6a. There is one real branch point due to collision with the second trajectory and a pair of complex conjugate points due to collisions with the fourth trajectory. From the previous discussion we know that after l_0 becomes larger than -3 the third trajectory has the limiting value l_0 for $k^2 \to -0$. This means that for smaller g, when l_0 is still less than -3, there already was in the plane of the third trajectory the N-sector. The corresponding situation is shown in Fig. 6b. The two additional, as compared with Fig. 6a, branch points came, apparently, from other sheets through the complex cuts of Fig. 6a.

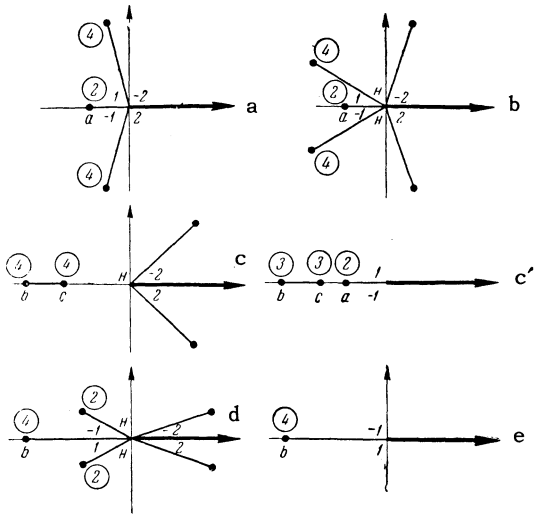

FIG. 6. Complex k^2 plane for the trajectory with n = 3 for various coupling constants; a – prior to the arrival of the N-pole; b – after the arrival of the N-pole for $l_0 < -3$; c – $l > -3$; c′ – real branch points of the fourth trajectory for the same coupling constants as in the case c; d – departure of branch points into the complex plane; e – final appearance of the complex plane after the passage of the N-pole. The points a, b and c correspond to the analogous points in Fig. 4.

At the moment when $l_0 = -3$ the pair of complex branch points of Fig. 6b arrive at the negative real axis. At that the real branch point due to collision with the second trajectory falls on the fourth sheet (i.e., as was previously explained, the second trajectory collides now with the fourth). As g is further increased the branch points diverge along the real axis (Fig. 6c), there being no cut between zero and the right branch point. For that same value of g the positions of the real branch points in the k^2 plane of the fourth trajectory are shown in Fig. 6c′.

With increasing g, as was already noted, the points a and c approach each other, coincide, and become complex. After that the k^2 plane for the third trajectory looks as shown in Fig. 6d. The conjugate branch points correspond to collision with the second trajectory. We should place these points in the plane of the third (and not fourth) trajectory because if we don't then the limiting value of the third trajectory for $k^2 \to -0$ would remain equal to l_0 whereas it is clear from the foregoing that it should be equal to $-\frac{1}{2}$.

As g is further increased pairs of complex branch points disappear in succession through the physical cut. At the moment when the branch points due to the second trajectory disappear there remains in the complex k^2 plane of the third trajectory only, aside from the physical cut, one real branch point (Fig. 6e) and the second trajectory becomes normal. With increasing g as the next N-pole passes through, the position of the singularities of the third trajectory undergoes the same changes as were previously described for the second trajectory. Thus with the passing of the first N-pole there disappears from the k^2 plane of the third trajectory a pair of complex branch points; the second N-pole sweeps the complex plane clean of the real branch point and thereafter the third trajectory also becomes normal.

It is easy to understand that an analogous process occurs also with the remaining trajectories: with increasing g, as N-poles pass through, the branch points in succession disappear through the physical cut and in the end the trajectories become normal. It is not hard to see that in this respect even the first pole (n = 1) is no exception. For repulsion (g < 0) this pole has a real branch point due to collision with the second. This point disappears onto an unphysical sheet through the point $k^2 = 0$ for g = 0.

We are grateful to V. N. Gribov for numerous and useful discussions, and also to I. T. Dyatlov for valuable to the authors criticism.

APPENDIX

POLE TRAJECTORY EQUATION FOR SMALL k^2

We have previously[1] derived the following exact equation for the trajectories of Regge poles:

$$\frac{e^{-i\pi\lambda}}{k}\int_0^\infty j_\lambda(kr)\,U(r)\,\psi_\lambda(r)\,dr = \sin\pi\lambda + \frac{1}{k}\int_0^\infty j_{-\lambda}(kr)\,U(r)\,\psi_\lambda(r)\,dr, \tag{A.1}$$

where $\lambda = l = 1/2$, $j_\lambda(x) = \sqrt{\pi x/2}\,J_\lambda(x)$, and the radial wave function $\psi(r)$ satisfies the integral equation

$$\psi_\lambda(r) = j_\lambda(kr) + \frac{1}{k\sin\pi\lambda}\int_0^r [j_\lambda(kr)\,j_{-\lambda}(kr') - j_{-\lambda}(kr)\,j_\lambda(kr')]\,U(r')\,\psi_\lambda(r')\,dr'. \tag{A.2}$$

In [1] j_λ and ψ_λ were denoted by j_l and ψ_l. For small k

$$j_\lambda(kr) \sim \frac{\sqrt{\pi}}{\Gamma(1+\lambda)}\left(\frac{kr}{2}\right)^{\lambda+1/2}. \tag{A.3}$$

Substituting Eq. (A.3) into (A.2) and expressing ψ_λ in the form

$$\psi_\lambda(r) \sim \frac{\sqrt{\pi}}{\Gamma(1+\lambda)}\left(\frac{kr}{2}\right)^{\lambda+1/2}\chi_\lambda(r), \tag{A.4}$$

we obtain for χ_λ the integral equation

$$\chi_\lambda(r) = 1 + \frac{1}{2\lambda}\int_0^r\left[1-\left(\frac{r'}{r}\right)^{2\lambda}\right]U(r')\,\chi_\lambda(r')r'\,dr'.$$

At that Eq. (A.1) takes on the form

$$\frac{e^{-i\pi\lambda}}{2}\frac{\pi}{[\Gamma(1+\lambda)]^2}\left(\frac{k^2}{4}\right)^\lambda\int_0^\infty r^{2\lambda}\,U(r)\,\chi_\lambda(r)\,r\,dr = \sin\pi\lambda\left[1+\frac{1}{2\lambda}\int_0^\infty U(r)\,\chi_\lambda(r)\,r\,dr\right]. \tag{A.6}$$

For the case of a Yukawa potential $U(r) = -2g\mu e^{-\mu r}/r$ under consideration Eq. (A.5) reduces to

$$\chi_\lambda(x) = 1 + \frac{g}{\lambda}\int_0^x e^{-x'}\left[\left(\frac{x'}{x}\right)^{2\lambda}-1\right]\chi_\lambda(x')\,dx', \qquad (x=\mu r), \tag{A.7}$$

and Eq. (A.6) to

$$g\frac{\sqrt{\pi}\,\Gamma(-\lambda)}{\Gamma\left(-\lambda+\frac{1}{2}\right)}\left(\frac{k^2}{\mu^2}e^{-i\pi}\right)^\lambda A(\lambda,g) = B(\lambda,g)\cos\pi\lambda,$$

where

$$A(\lambda,g) = \int_0^\infty e^{-x}\chi_\lambda(x)\,x^{2\lambda}\,dx/\Gamma(2\lambda+1),$$

$$B(\lambda,g) = 1 - (g/\lambda)\int_0^\infty e^{-x}\chi_\lambda(x)\,dx. \tag{A.8}$$

Integrating Eq. (A.7) and substituting the result into Eq. (A.8) we obtain $A(\lambda,g)$ and $B(\lambda,g)$ in the form of power series:

$$A(\lambda,g) = \sum_{n=0}^\infty a_n\left(-\frac{g}{\lambda}\right)^n, \quad B(\lambda,g) = \sum_{n=0}^\infty b_n\left(-\frac{g}{\lambda}\right)^n. \tag{A.9}$$

The first coefficients in these series are equal to

$$a_0 = 1, \quad a_1 = a_0 - 2^{-2\lambda},$$

$$a_2 = -\frac{a_0}{2} + a_1 + \frac{3^{-2\lambda+1}}{4} - \int_1^3\frac{dyy^{-2\lambda}}{(y+1)^2},$$

$$a_3 = \frac{a_0}{6} - \frac{a_1}{2} + a_2 - \frac{4^{-2\lambda+1}}{9} - 2\int_1^4\frac{dyy^{-2\lambda}}{(2y+1)^2} + 2\int_1^4\frac{dyy^{-2\lambda}}{(y+2)^2} + 2\int_2^4\frac{dyy^{-2\lambda}}{(y+2)^2}, \tag{A.10}$$

$$b_0 = 1, \quad b_1 = b_0, \quad b_2 = -\frac{b_0}{2} + b_1 - \frac{2\pi\lambda}{\sin 2\pi\lambda} + \int_0^1\frac{dyy^{-2\lambda}}{(y+1)^2},$$

$$b_3 = \frac{b_0}{6} - \frac{b_1}{2} + b_2 - \frac{2\pi\lambda}{\sin 2\pi\lambda}(2^{-2\lambda} - 2^{2\lambda}) + 2\int_0^1\frac{dyy^{-2\lambda}}{(2y+1)^2} - 2\int_0^1\frac{dyy^{-2\lambda}}{(y+2)^2}. \tag{A.11}$$

The coefficients b_n in Eq. (A.11) are given in a form convenient for use in the left half-plane Re $\lambda < 0$. The b_i ($i \geq 2$) have poles at all integer and half-integer negative points. For half-integer λ these poles are compensated by zeros of the cosine in Eq. (A.8). In the neighborhood of integer λ (i.e., half-integer l) the indicated singularities reflect the illegitimacy of the utilized asymptotic behavior [Eq. (A.3)] of the Bessel functions; near these points Eqs. (A.6) and (A.8) are inapplicable. As was shown in the Appendix in [1] the region of inapplicability of the equations has dimensions of order g.

One arrives at Eq. (11) of the text if one keeps only first order expressions for the functions $A(\lambda,g)$ and $B(\lambda,g)$, i.e., keeps only a_0, a_1, b_0, b_1.

[1] Azimov, Ansel'm, and Shekhter, JETP (in press).

[2] Ahmadzadeh, Burke, and Tate, preprint UCRL-10216.

Translated by A. M. Bincer
172